NASA/TM—2018-220008

Fatigue Life of a NiCr-Coated Powder Metallurgy Disk Superalloy After Varied Processing and Exposures

Timothy P. Gabb and James A. Nesbitt
Glenn Research Center, Cleveland, Ohio

Derek Hass
Directed Vapor Technologies, Charlottesville, Virginia

Jack Telesman, Susan L. Draper, Bernadette J. Puleo, and Richard B. Rogers
Glenn Research Center, Cleveland, Ohio

Robert A. Miller
Vantage Partners, LLC, Brook Park, Ohio

November 2018

NASA STI Program . . . in Profile

Since its founding, NASA has been dedicated to the advancement of aeronautics and space science. The NASA Scientific and Technical Information (STI) Program plays a key part in helping NASA maintain this important role.

The NASA STI Program operates under the auspices of the Agency Chief Information Officer. It collects, organizes, provides for archiving, and disseminates NASA's STI. The NASA STI Program provides access to the NASA Technical Report Server—Registered (NTRS Reg) and NASA Technical Report Server—Public (NTRS) thus providing one of the largest collections of aeronautical and space science STI in the world. Results are published in both non-NASA channels and by NASA in the NASA STI Report Series, which includes the following report types:

- TECHNICAL PUBLICATION. Reports of completed research or a major significant phase of research that present the results of NASA programs and include extensive data or theoretical analysis. Includes compilations of significant scientific and technical data and information deemed to be of continuing reference value. NASA counter-part of peer-reviewed formal professional papers, but has less stringent limitations on manuscript length and extent of graphic presentations.

- TECHNICAL MEMORANDUM. Scientific and technical findings that are preliminary or of specialized interest, e.g., "quick-release" reports, working papers, and bibliographies that contain minimal annotation. Does not contain extensive analysis.

- CONTRACTOR REPORT. Scientific and technical findings by NASA-sponsored contractors and grantees.

- CONFERENCE PUBLICATION. Collected papers from scientific and technical conferences, symposia, seminars, or other meetings sponsored or co-sponsored by NASA.

- SPECIAL PUBLICATION. Scientific, technical, or historical information from NASA programs, projects, and missions, often concerned with subjects having substantial public interest.

- TECHNICAL TRANSLATION. English-language translations of foreign scientific and technical material pertinent to NASA's mission.

For more information about the NASA STI program, see the following:

- Access the NASA STI program home page at http://www.sti.nasa.gov

- E-mail your question to help@sti.nasa.gov

- Fax your question to the NASA STI Information Desk at 757-864-6500

- Telephone the NASA STI Information Desk at 757-864-9658

- Write to:
  NASA STI Program
  Mail Stop 148
  NASA Langley Research Center
  Hampton, VA 23681-2199

NASA/TM—2018-220008

Fatigue Life of a NiCr-Coated Powder Metallurgy Disk Superalloy After Varied Processing and Exposures

Timothy P. Gabb and James A. Nesbitt
Glenn Research Center, Cleveland, Ohio

Derek Hass
Directed Vapor Technologies, Charlottesville, Virginia

Jack Telesman, Susan L. Draper, Bernadette J. Puleo, and Richard B. Rogers
Glenn Research Center, Cleveland, Ohio

Robert A. Miller
Vantage Partners, LLC, Brook Park, Ohio

National Aeronautics and
Space Administration

Glenn Research Center
Cleveland, Ohio 44135

November 2018

Acknowledgments

The authors would like to acknowledge Don Humphrey and John Setlock of Zin Technologies, Inc. for heat treating all specimens, Rick Paul of wetblasting.com for wet blasting selected specimens, and Laura Evans for reviewing this manuscript.

This work was sponsored by the Advanced Air Vehicles Program (AAVP), Advanced Air Transport Technology (AATT) Project at the NASA Glenn Research Center

Level of Review: This material has been technically reviewed by technical management.

Available from

NASA STI Program
Mail Stop 148
NASA Langley Research Center
Hampton, VA 23681-2199

National Technical Information Service
5285 Port Royal Road
Springfield, VA 22161
703-605-6000

This report is available in electronic form at http://www.sti.nasa.gov/ and http://ntrs.nasa.gov/

Fatigue Life of a NiCr-Coated Powder Metallurgy Disk Superalloy After Varied Processing and Exposures

Timothy P. Gabb and James A. Nesbitt
National Aeronautics and Space Administration
Glenn Research Center
Cleveland, Ohio 44135

Derek Hass
Directed Vapor Technologies
Charlottesville, Virginia 22903

Jack Telesman, Susan L. Draper,* Bernadette J. Puleo, and Richard B. Rogers
National Aeronautics and Space Administration
Glenn Research Center
Cleveland, Ohio 44135

Robert A. Miller
Vantage Partners, LLC
Brook Park, Ohio 44142

Abstract

A protective ductile NiCr coating has shown promise to mitigate oxidation and corrosion attack on superalloy disk alloys. The effects of this coating on fatigue life and failure modes of the disk superalloy are an important concern. The objective of this study was to investigate the fatigue life and failure modes of disk superalloy specimens protected by this coating, using varied pre-coating and post-coating processes. Cylindrical gage fatigue specimens of a powder metallurgy-processed disk superalloy were grit blast or wet blast before being coated with a ductile NiCr coating, then shot peened at low or medium levels after coating. All were then heat treated, some exposed, and finally all were subjected to fatigue at high temperature. The effects of varied pre-coating treatment, post-coating shot peening, and oxidation plus hot corrosion exposures on fatigue life with the coating were compared.

Introduction

Disk application temperatures of 700 °C and higher can enhance oxidation and also activate hot corrosion attack modes in harmful environments (Ref. 1). These damage modes could then become important limitations on fatigue durability. Protective metallic coatings are needed to mitigate this damage.

Several studies have shown that oxidation from exposures at 700 °C and higher can impair the fatigue resistance of disk superalloys (Refs. 2 to 4). This oxidation can include the formation of oxide layers, as well as related changes in superalloy chemistry and phases adjacent to the oxide layers. Of the oxide layers, the formation of chromium oxide is known to be protective, however, other nickel, cobalt, and titanium oxides can also form that are not protective. Nearby, selective oxidation of certain elements can result in the formation of a zone adjoining the oxide layers that is only made up of weakened gamma phase, without gamma prime precipitates. This zone can sometimes also be recrystallized to a finer grain size than the original disk alloy grains. Furthermore, due in part to a lack of $M_{23}C_6$ carbides, the grain

*Retired

boundaries in this zone can be susceptible to cracking during fatigue at high temperatures. Collectively, these aspects of oxidation can lower the fatigue life of disk superalloys up to 98% (Ref. 4).

Independently, Type II hot corrosion attack can occur near 700 °C and higher on superalloy surfaces (Refs. 5 and 6) by the melting of accumulated deposits containing mixtures of sodium-, magnesium-, and calcium- sulfates, as well as by direct impingement of SO_2-containing exhaust gas. Here, the liquid sulfates can react with surface oxides to make them no longer protective. This allows attack of the newly exposed superalloy surface. The grain boundaries can be preferentially attacked for certain conditions. Pits can form in some conditions, while general corrosion can otherwise occur (Ref. 7). The pits can act as geometric stress concentration sites, which encourage cracks to initiate during mechanical fatigue loading. The oxide layers within pits are also not fatigue resistant or protective, allowing further penetration of pits and fatigue cracking. Pitting and uniform corrosion can also reduce the fatigue life of disk superalloys up to 98% (Refs. 3, 8 to 11).

A suitable metallic coating could provide protection of exposed superalloy surfaces from this oxidation and corrosion. While PtAl, NiAl, and NiCoCrAlY (Ref. 12) coatings have been extensively developed to protect superalloy airfoils from oxidation and corrosion, these coatings have lower ductility and fatigue resistance than turbine disk superalloys. A more suitable coating is necessary that would have minimal effects on the fatigue resistance of the disk surfaces upon which it is applied, as disks are fracture critical in aero-propulsion applications.

Before coating, the surface of the superalloy needs to be cleaned. Roughening of the surface can also be very beneficial for certain types of coating deposition to help improve adherence of the coating. Grit blasting, in which alumina grit particles are directed in an air stream at elevated pressure, has often been used on superalloy airfoils before coating (Ref. 12), particularly overlay MCrAlY-type coatings. Yet, other processes could be viable, in which alumina, silica, or other hard grit particles are directed in carrier streams at elevated pressure onto the surface to be cleaned. It is unclear which among these “pre-coating” surface treatments could be more beneficial for disk superalloys before coating. However, it has been demonstrated that such nonmetallic particles, if embedded at the surface of powder metallurgy disk superalloys, can reduce fatigue resistance by prematurely initiating fatigue cracks (Ref. 13). This suggests such “pre-coating” surface treatments should be screened before application to disk superalloys.

In addition to pre-coat processes, post-coat processing could also have a significant effect on the LCF life of a coated component. Shot peening is routinely used to produce a consistent surface finish and impart beneficial compressive residual stresses near the treated surfaces, and can impede fatigue cracking there (Refs. 14 and 15). Therefore, many turbine disk surfaces, after being machined using various process (Ref. 16), are subsequently shot peened. To take advantage of this, a protective coating could be applied after fully machining a disk surface after which the coated surfaces could then be shot peened. The residual stresses, roughness, and fatigue life before and after exposures of such coated and shot peened surfaces would need to be considered for such an approach, in order to assure the coating’s effectiveness. Yet, it is unclear what shot peening intensity and coverage would be more beneficial as a “post-coating” surface treatment for disk superalloys after coating.

A baseline disk coating process with grit blasting as the pre-coating treatment and shot peening at 16 N–200% as the post-coating treatment was applied using a Ni45CrY $\gamma + \alpha$ phase coating on a disk superalloy (Ref. 17). In screening tests, the coated specimens had fatigue lives comparable to uncoated specimens. After oxidation plus hot corrosion, these coated specimens had improved fatigue lives in comparison to uncoated specimens. However, enhanced fatigue cracking was observed at the coated surface of specimens with and without the environmental exposures. This could be related to the coating ductility and strength, as well as the selected pre-coating and post-coating process conditions.

The objective of this study was to investigate the effects of alternative pre-coating and post-coating processes on fatigue life and failure modes of a disk superalloy protected by a more ductile, γ phase Ni29Cr coating. Baseline and alternative surface blasting treatments were assessed before coating, then baseline and alternative shot peening conditions were assessed after coating. The responses of roughness, residual stress, corrosion pitting resistance, and fatigue life were then assessed.

Materials and Procedure

The low solvus high refractory (LSHR) powder metallurgy disk superalloy test material had the composition listed in weight percent of 3.54Al-0.027B-0.045C-20.4Co-12.3Cr-0.1Fe-2.71Mo-1.49Nb-0.02O-0.012Si-1.52Ta-3.45Ti-0.01V-4.28W-0.049Zr-bal. Ni. The LSHR superalloy powder was atomized in argon, consolidated by hot isostatic pressing, extruded, and isothermally forged into flat disks. Extracted rectangular blanks about 14 mm square and 55 mm long were consistently supersolvus solution heat treated at 1171 °C for 2 h and subsequently aging heat treated at 855 °C for 4 h, followed by 775 °C for 8 h. The resulting LSHR microstructure (Fig. 1) had an average linear intercept grain size of about 15 μm.

Fatigue specimens having uniform gage sections 6.4 mm in diameter were then machined to the dimensions shown in Figure 2. The test specimens were all machined by low stress grinding, followed by longitudinal polishing with abrasive paper to a root mean square roughness of less than 0.2 μm. However, before coating, the gage surfaces of all specimens were "pre-conditioned". A large group of specimens were pre-conditioned by grit blasting, using –220 mesh alumina grit. The surfaces of a smaller group were later pre-conditioned by wet blasting, using 15% of –300 mesh silica glass beads. A third small group of specimens had the grit blasting followed by the wet blasting treatments.

A Directed Vapor Deposition (DVD) approach was employed by Directed Vapor Technologies International, Inc. to apply the coating. Both ends of each specimen were held and shielded in a metal fixture, so that only the reduced gauge test section was exposed for coating. The fixture was rotated during the coating process to enable production of a uniform coating thicknesses on the individual

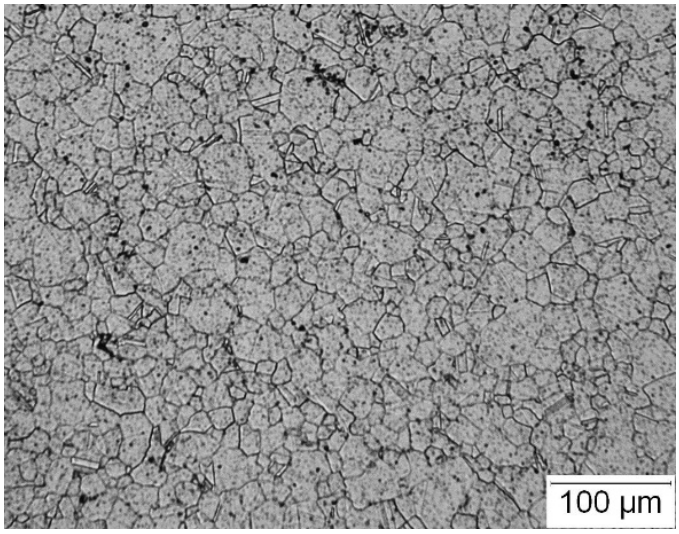

Figure 1.—Microstructure of powder metallurgy superalloy LSHR.

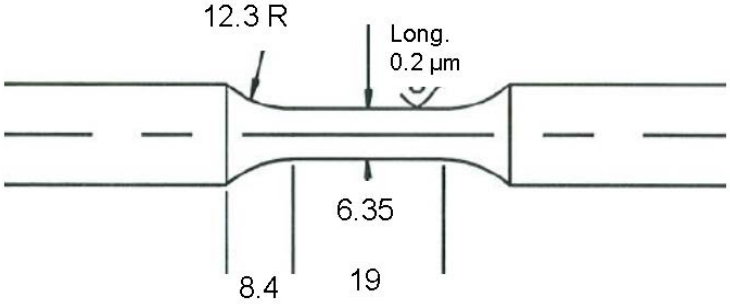

Figure 2.—Fatigue specimen gage section, with dimensions in mm.

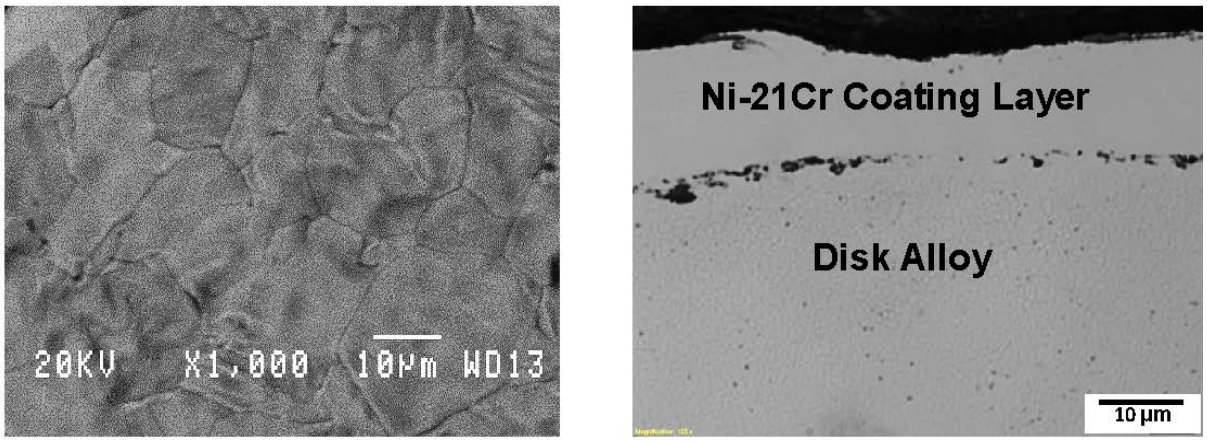

(a) (b)

Figure 3.—Coated superalloy. (a) As-coated surface. (b) Cross-section of coated plus shot peened plus heat treated fatigue specimen.

samples. Four bars were thereby coated during a single coating run. Several coating runs were performed using the same process settings. The typical microstructure of the coating after application and subsequent shot peening at 16 N-200% and heat treatment is shown in Figure 3. The black inclusions at the coating/substrate interface are embedded alumina grit particles, which will be discussed later. The coating composition was measured by electron dispersive spectroscopy (EDS) in a scanning electron microscope (SEM) to be Ni-21Cr in weight percent. The coating had a mean thickness of 23.1 μm with a 95% confidence interval of ±2.2 μm for the unexposed specimens, using measurements of their fracture surfaces adjacent to the failure initiation point. It consisted of a single nickel-rich γ phase. The mean linear intercept grain size of the coating measured normal to the specimen surface and environment was 12 μm.

Uncoated and coated fatigue test specimens were shot peened at Curtiss-Wright, Metal Improvement Division using conditioned cut stainless steel wire (CCW14), in accordance with AMS2432 specifications. A large group of specimens were shot peened at 16 N intensity and coverage 200%. A second group of specimens was later shot peened at a lower intensity of 8 N and lower coverage of 150%. Here, 100% coverage indicates 100% of the surface area has been impacted, while 200% indicates double the amount of time of shot peening needed to attain this 100% of coverage (Ref. 18) was employed. After shot peening, all test specimens were heat treated at 760 °C for 8 h to promote inter-diffusion between the coating and substrate for the coated specimens, and to help form a protective chromium-oxide layer on the surface. This heat treatment was consistently performed at a low partial pressure of oxygen calculated to be 1×10^{-16} MPa, intended to encourage Cr_2O_3 formation and growth (Ref. 17).

Residual stresses were measured on the gage surface before exposures using a Bruker D8 Discover (area detector) x-ray diffractometer aligned in accordance with the approach and error bounds specified in ASTM E 915-10, but applied to the side-inclination rather than iso-inclination method. Data was gathered using Mn Kα radiation and the (311) crystallographic plane on a specimen target area of 1.2 mm^2 (Ref. 20). These x-ray results were analyzed using the Bruker LEPTOS v.7 software. Average roughness was measured using a Zygo NewView 7200 optical measurement system having a resolution of 0.001 μm.

Selected coated and uncoated specimens were exposed to oxidation followed by hot corrosion before fatigue testing. Oxidation was first performed in air at 760 °C for 500 h. These oxidized specimens were then coated with a salt mixture of 59 wt% Na_2SO_4 and 41 wt% $MgSO_4$ applied at approximately 2 mg/cm^2. This salt lies at a eutectic composition with a melting point of 662 °C and was observed to melt and flow in previous testing at 760 °C. They were then suspended horizontally in a resistance-heating

tube furnace at 760 °C in air for 50 h. Previous work demonstrated that uncoated LSHR test specimens corrosion treated in this manner and tested at 760 °C in air nucleated and grew corrosion pits within just 24 h, which had a substantial effect on fatigue lives (Ref. 19). One additional pair of coated specimens were oxidized and corroded for these times at 815 °C, in order to screen the effects of increasing exposure temperature.

Fatigue cycling was conducted using a servo-hydraulic test machine with a resistance heating furnace that enclosed the specimen and specimen grips. Stress was consistently cycled between maximum and minimum stress values of 841 and –427 MPa in each cycle using a saw-tooth waveform at a frequency of 0.33Hz. These stresses corresponded to the stabilized maximum and minimum stresses produced by tests run on this material with strain cycled at a strain range of 0.76% and strain ratio (minimum/maximum strain) of 0 at 760 °C. However, no extensometer contacted the coating in the present tests.

Selected fatigue specimens were examined after preparation, and after the oxidation plus corrosion exposures. All test specimens were later examined after fatigue cycling to failure. Fracture surfaces were examined using a JEOL 6100 scanning electron microscope (SEM). Actual coating thickness was measured at this point adjacent to the dominant crack causing failure on unexposed coated fatigue specimen's fracture surfaces. The side of the specimen gage was then consistently imaged in the SEM adjacent to the main fatigue crack causing failure, to assess secondary fatigue cracks that had been unloaded during growth of the main crack.

Results and Discussion

Baseline Coating Process - Grit Blast + Coat + 16 N-200% + Heat Treated 760 °C for 8 h

Specimen Surface Conditions

Uncoated specimen gage surfaces after grit blasting are shown in Figure 4(a). The grit blast surface had a finely textured, roughly scalloped appearance. An area fraction of 0.034 alumina grit particles up to 10 μm in diameter was embedded in the grit blast surface. Deposition of the coating gave a fine texture that was generally nodular, shown in Figure 4(b). More prominent nodules known as spits were also observed, sometimes produced during this coating process. The shot peened and heat treated surfaces were more fairly uniform, with the formerly grooved and nodular surface textures mostly eliminated, being replaced with an undulating, dimpled texture, as shown in Figure 4(c). Shot peening of the coated surface flattened the spits, and resulted in folds of metal ("laps") sometimes occurring at the edges of dimples created by the impact of shot. As shown in Figure 5, both measured average roughness and peak-valley roughness increased between grit blasting and the final coated, shot peened, and heat treated condition. While the coating had a mean thickness of 23.1 μm for the unexposed specimens, measurements of fracture surfaces adjacent to the failure initiation point indicated the coating thickness typically varied with a 95% confidence interval of 2.2 μm around the mean, due in part to the shot peening.

Residual stresses measured at the surfaces are shown in Figure 6. Residual stresses changed significantly for each processing step between grit blasting and final heat treatment. Uncoated grit blast surfaces had compressive residual stresses exceeding –1,100 MPa. But the applied coating had a low tensile residual stress near 250 MPa. Shot peening at 16 N-200% restored the compressive residual stress at the coated surface to initial grit blast levels. Yet, the final step of heat treatment at 760 °C for 8 h relaxed the compressive residual stresses at the coated surface, back to the low tensile levels previously measured as-coated. The generation of compressive residual stresses in the coating by shot peening has been described for MCrAlY coatings applied on superalloys in general by several processes (Ref. 20) and for NiCr coatings on disk superalloys (Ref. 21). The complete relaxation in the coating of these compressive stresses during subsequent heat treatment at the high temperature used in the present study had been previously observed for a Ni45CrY $\gamma + \alpha$ phase coating applied on LSHR (Ref. 22). This response of such coatings appears to be related to their low stress relaxation resistance.

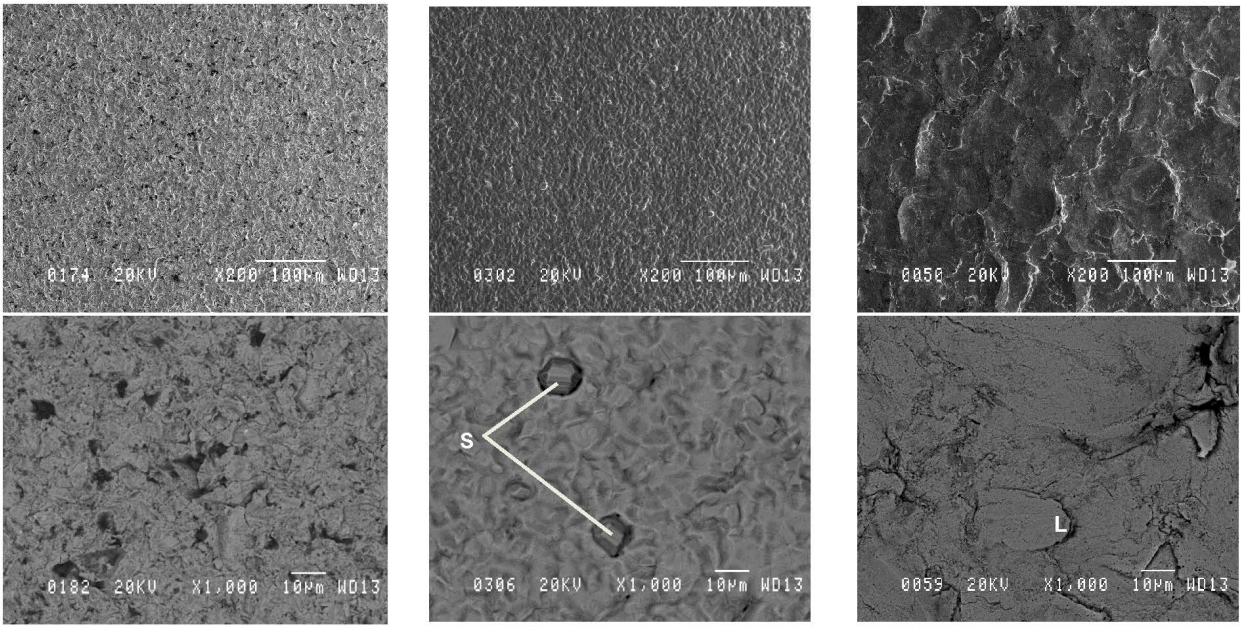

(a) (b) (c)

Figure 4.—Effects of baseline specimen preparation steps on surface conditions. (a) Grit blast, showing embedded alumina grit (black particles). (b) Coated, showing spits (S). (c) Shot peened 16 N-200% and heat treated 760 °C for 8 h, showing laps (L). The fatigue loading direction is oriented vertically.

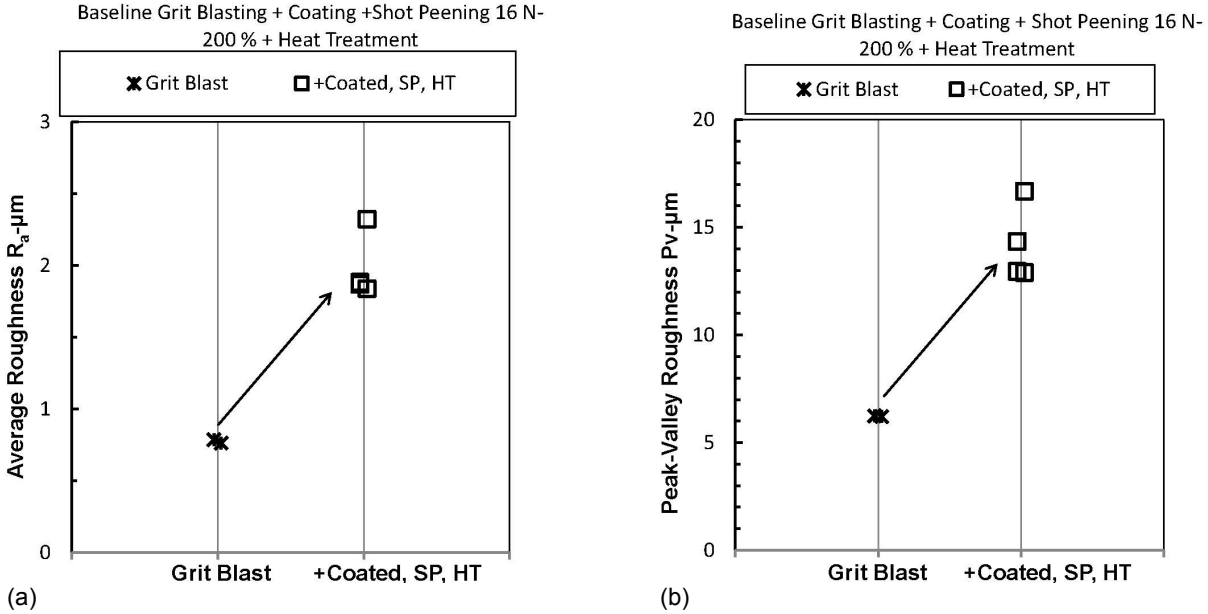

(a) (b)

Figure 5.—Roughness after grit blasting, and after subsequent coating, shot peening, plus heat treatment. (a) Average roughness. (b) Peak-valley roughness. The hollow symbols are for coated specimens.

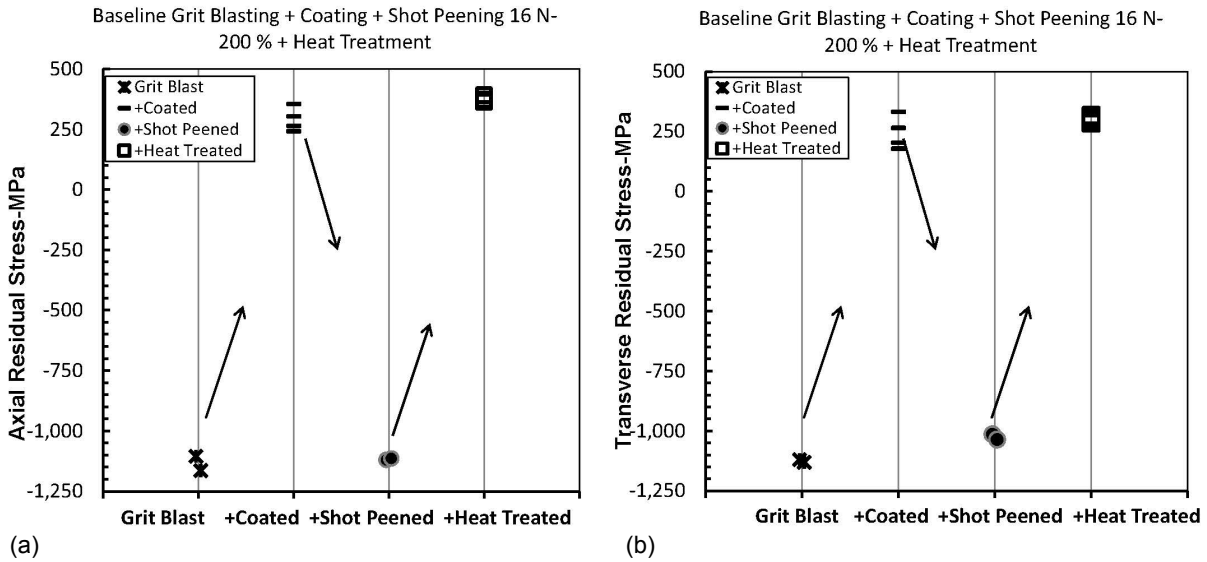

Figure 6.—Residual stresses measured at the surface after successive baseline processing steps. (a) Axial direction parallel to the fatigue load. (b) Transverse direction.

Fatigue Lives and Failure Modes

Fatigue lives are compared for uncoated specimens and those coated using the baseline process, before and after combined oxidation plus corrosion exposures, in Figure 7. Coated specimens prepared using the baseline process had comparable mean fatigue lives to uncoated specimens. However, the combined oxidation plus corrosion exposures significantly reduced fatigue life for both uncoated and coated specimens. The coating using the baseline process gave a modest benefit in life over uncoated specimens after oxidation plus corrosion at 760 °C. However, exposures at 815 °C reduced coated fatigue lives from near 50,000 cycles after exposures at 760 °C, to about 10,000 cycles after exposures at 815 °C.

The associated failure modes are compared in Figure 8. Uncoated specimens that were not exposed failed from single transgranular cracks initiated at the surface from shot peened dimples, or initiated internally at nonmetallic inclusions. Only a very few fatigue cracks less than 15 μm wide were observed on the side of the gage surface adjacent to the main fatigue crack causing failure. Coated specimens that were not exposed usually failed from multiple transgranular fatigue cracks initiated in the coating along the shot peened surface. A dense network of fatigue cracks that were typically 50 to 350 μm wide were observed on the side of the coated gage surface adjacent to the main fatigue crack causing failure.

The effects of combined oxidation plus corrosion on failure mode varied between uncoated and coated specimens. Uncoated specimens that were oxidized 500 h plus corroded 50 h at either 760 °C or 815 °C failed from multiple intergranular surface cracks initiated at corrosion pits. The corrosion pits initiating cracks on the fracture surface had widths of 15 to 75 μm, and depths of 10 to 30 μm. However, some cracks also initiated where two adjacent pits joined or were very closely separated, as observed in prior similar studies (Ref. 11). Additional intergranular fatigue cracks were observed to initiate on the side of the gage surface adjacent to the main fatigue crack causing failure, at other corrosion pits.

Coated specimens did not have corrosion pits exposing the substrate superalloy. Yet, some surface oxidation and corrosion of the coating was apparent, and fatigue failures still initiated from multiple elongated cracks initiated at the surface of the coating. The cracks initially grew with a mixed intergranular-transgranular mode in the LSHR, but transitioned to a predominantly transgranular crack growth mode after growing less than about 20 μm. These side cracks often occurred where darker patches imaged in backscatter SEM images indicated deeper oxidation and corrosion of the coating.

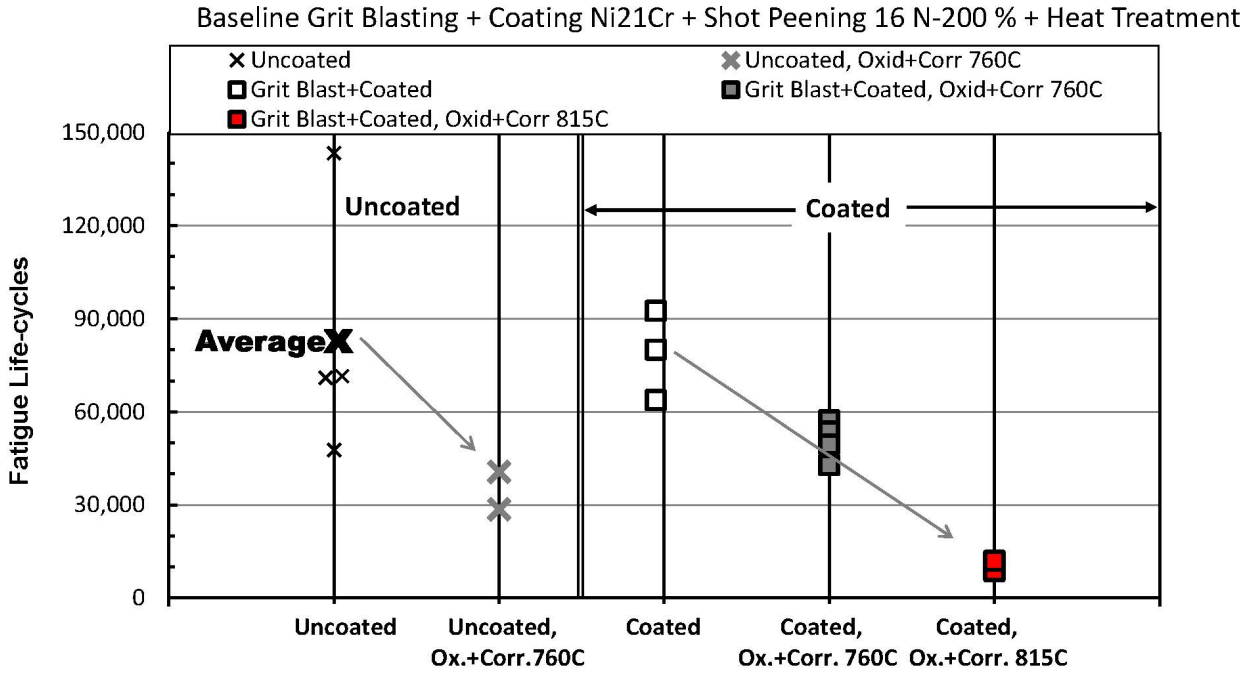

Figure 7.—Comparison of fatigue lives for uncoated versus coated specimens prepared using the baseline process.

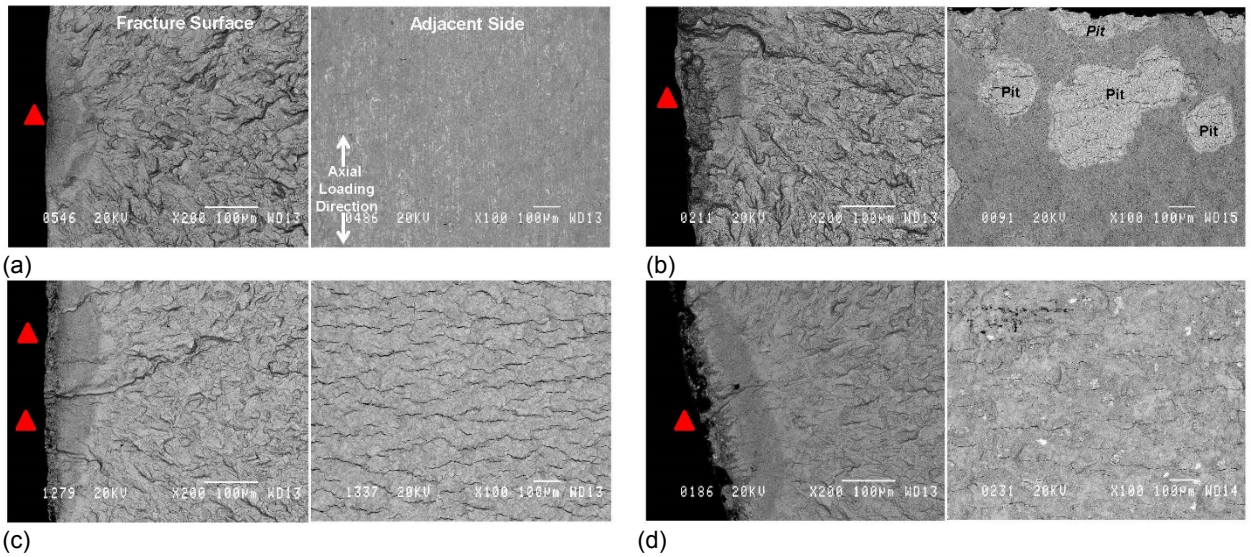

Figure 8.—Fatigue failure modes for uncoated versus coated specimens prepared using the baseline process. (a) Uncoated, unexposed. (b) Uncoated, oxidized plus corroded. (c) Coated, unexposed. (d) Coated, oxidized plus corroded.

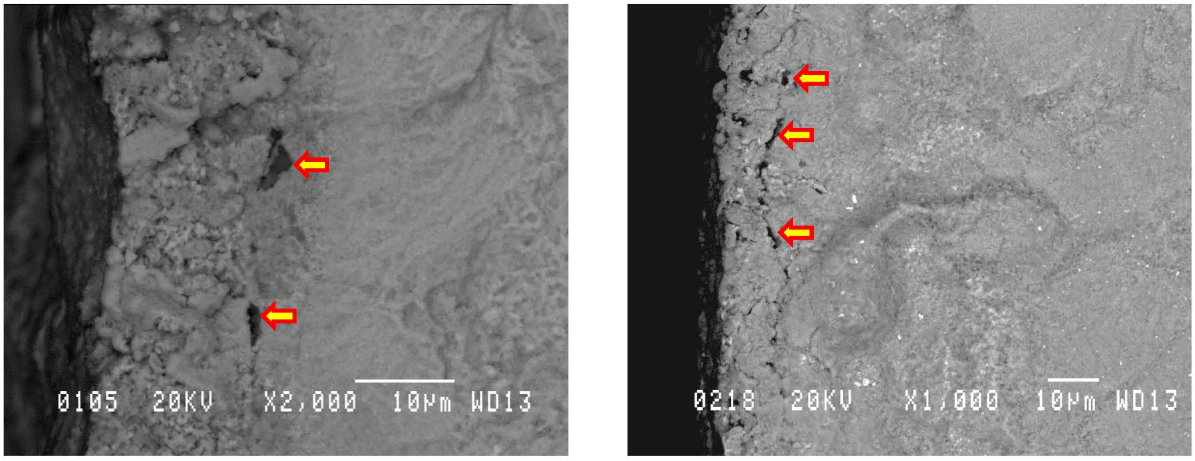

(a) (b)

Figure 9.—Cracks on the fracture surfaces of coated specimens, with arrows showing exposed alumina grit blasting particles embedded at the coating-substrate interface. (a) Unexposed. (b) Oxidized plus corroded.

While the single γ phase Ni21Cr alloy used as the present coating is known to have higher ductility than the γ + α phase Ni45CrY studied earlier (Ref. 22) or other MCrAlY coatings (Ref. 12), all these coatings have lower reported strengths than typical powder metallurgy disk superalloys, predominantly made up of γ phase strengthened by 40 to 55% of γ' phase precipitates (Ref. 1). The lower strength of these coatings could help explain their enhanced fatigue cracking in comparison to the uncoated disk superalloy. Yet, the actual strength and ductility of the applied, shot peened, and heat treated coating used here could not be easily assessed. Graded coating layers with potentially varied phase compositions (Ref. 22), could result from the application process, and subsequent interdiffusion between the coating and substrate during subsequent processing, potential exposures, and fatigue testing. Of these, even the first steps of specimen preparation and application of the coating onto the superalloy could introduce impurities and foreign particles.

It was noted that cracks on the fracture surface sometimes uncovered alumina particles located at the coating-substrate interface, as shown in Figure 9. It was apparent that these particles had been embedded during the grit blasting process before coating, as shown in Figure 4(a). The role of these alumina particles in encouraging fatigue crack initiation in the tested specimens was unclear, as they were not always observed at fatigue cracks on the fracture faces examined. Yet, these particles at the coating-substrate interface have been reported to initiate fatigue cracks in disk superalloys (Ref. 13), and could be considered as potential contributors to the enhanced fatigue cracking of the coating. Hence, an alternative pre-treatment before coating that reduced or eliminated such contamination was investigated.

Alternative Pre-Coating Treatment—Wet Blasting

Surface Conditions

"Wet blasting" also directs abrasive particles in a pressurized stream to abrade a surface, but uses water as a carrying fluid to potentially give more uniform flow of the particles and soften the impacts of abrasive particles (Ref. 23). Depending on process conditions, this process could affect the amount of particles embedded in the surface, surface finish, and residual stresses in comparison with the baseline grit blasting. Hence, additional fatigue specimens were wet blast using 15% of 300 mesh silica glass beads at a pressure of 550 kPa. Typical fatigue specimen surfaces are compared in Figure 10 after wet blasting or baseline grit blasting, both as-blasted and after subsequent coating, shot peening, and heat treatment. The wet blast surface clearly had a lower extent of embedded particles than for the baseline grit blasting. Wet blast surfaces had 0.6 area percent of embedded silica particles up to 12 μm in maximum exposed dimension, versus 3.4 area percent of embedded alumina grit particles up to 10 μm in diameter

measured for grit blasting. The wet blast surfaces also had a lower average roughness Ra of 0.51 μm in comparison to 0.77 μm for the baseline grit blast surfaces, shown in Figure 11(a). Yet, axial residual stresses measured on the blasted surfaces were comparable, as shown in Figure 11(b). Ultimately, the wet and grit blast specimen surfaces were indistinguishable, after coating, shot peening at 16 N-200%, and heat treatment at 760 °C for 8 h, also compared in Figures 10 and 11. Surface appearance, average roughness, and axial residual stresses were not significantly affected by the alternate pre-treatment of wet blasting. Several other fatigue specimens were subjected to grit blasting followed by wet blasting, in search of additive effects. These "grit+wet blast" specimens also had appearance, roughness, and surface residual stress values indistinguishable from the above specimens, after coating, shot peening, and heat treatment.

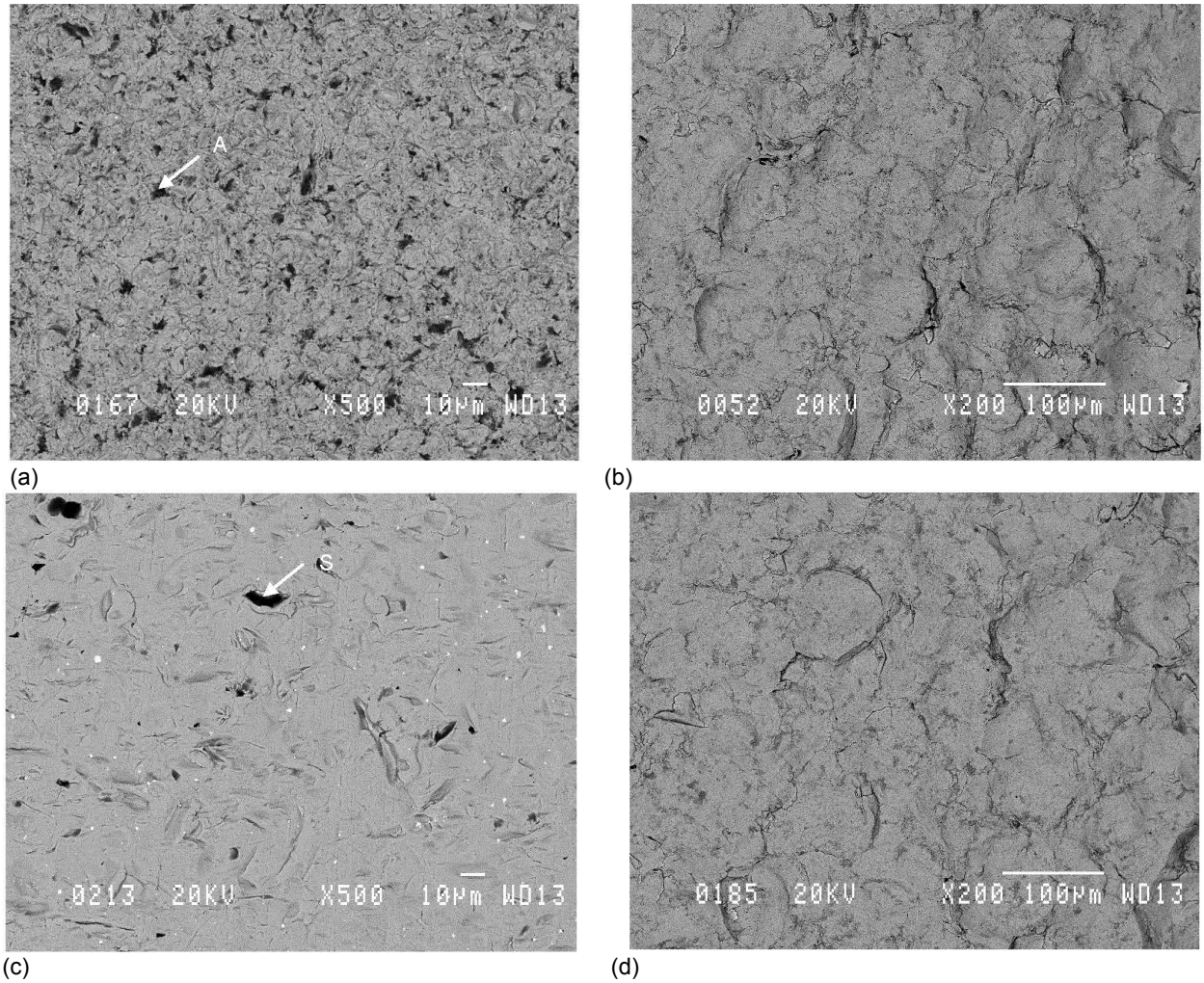

Figure 10.—Comparison of specimen surfaces for baseline grit blast to alternative wet blast pre-treatments. (a) Grit blast with 3.4 area percent of embedded aluminum oxide (A) particles. (b) Grit blast, coated, shot peened 16 N-200%, and heat treated. (c) Wet blast with 0.6 area percent of embedded silica (S) particles. (d) Wet blast, coated, shot peened 16 N-200%, and heat treated. The fatigue loading direction is oriented vertically.

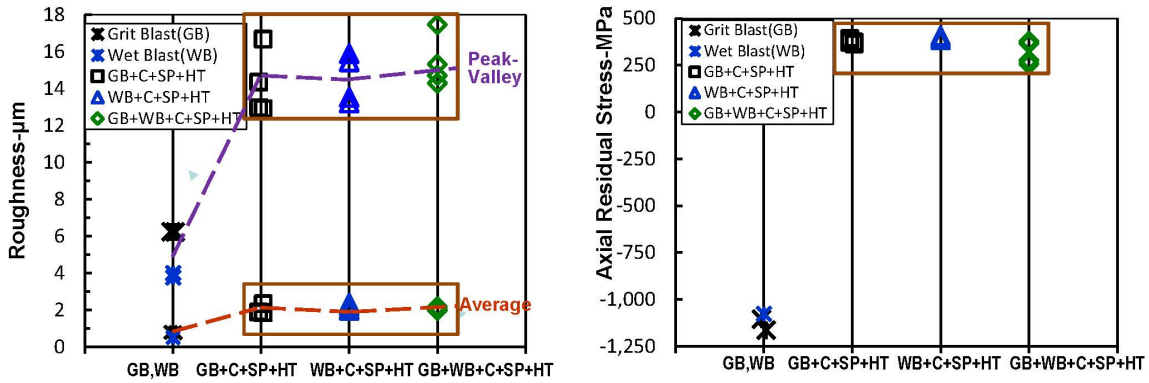

Figure 11.—Comparison of specimen surfaces'. (a) Roughness. (b) Axial residual stress for baseline grit blast and alternative wet blast pre-treatments: grit blast (GB); grit blast, coated, shot peened 16 N-200%, and heat treated (GB+C+SP+HT); wet blast (WB); wet blast, coated, shot peened 16 N-200%, and heat treated (WB+C+SP+HT).

Fatigue Lives and Failure Modes

Fatigue lives are compared in Figure 12 for grit blast, wet blast, and grit+wet blast specimens that were subsequently coated, shot peened 16 N-200%, heat treated at 760 °C for 8 h, and then fatigue tested, without oxidation plus corrosion exposures. Specimens prepared using only the wet blasting pre-treatment before coating had highest mean fatigue life.

The associated failure modes are compared in Figure 13. Coated specimens usually failed from multiple transgranular fatigue cracks initiated in the coating along the shot peened surface, for all of the pre-treatments applied. A dense network of fatigue cracks that were typically 28 to 424 µm wide were again observed on the side of the coated gage surface adjacent to the main fatigue crack causing failure.

These results indicated a pre-treatment was clearly beneficial for fatigue life of these coated specimens. Yet, the persistence of increased coating fatigue cracking even for the significantly lower content of grit particles embedded by the wet blasting process suggested the cracking was not strongly correlated to these particles. Applying both grit blasting and then wet blasting also indicated there was not a clear relationship to the enhanced fatigue cracking observed here.

It was noted that the shot peening at 16 N-200% significantly increased roughness and compressive residual stresses in the coating, through plastic deformation at the surface, evident in Figure 4. Yet, this could have produced significant deformation damage in the formerly ductile coating, to lower the coating's resistance to fatigue cracking. Therefore, a less intense shot peening process after the coating application was investigated.

Alternative Post-Coating Shot Peening—8 N-150%

Surface Conditions

The surface conditions are compared in Figure 14 for coated specimens shot peened at 8 N-150% versus the baseline 16 N-200%. These surfaces were generally similar in overall appearance, with an undulating, dimpled texture. Shot peening at 8 N-150% still produced dimples with laps. However, the lap heights and dimple depths were moderated in comparison to the baseline 16 N-200% condition. Average roughness and peak-valley roughness were each reduced about 40% for coated specimens given the alternative 8 N-150% shot peening conditions, as shown in Figure 15.

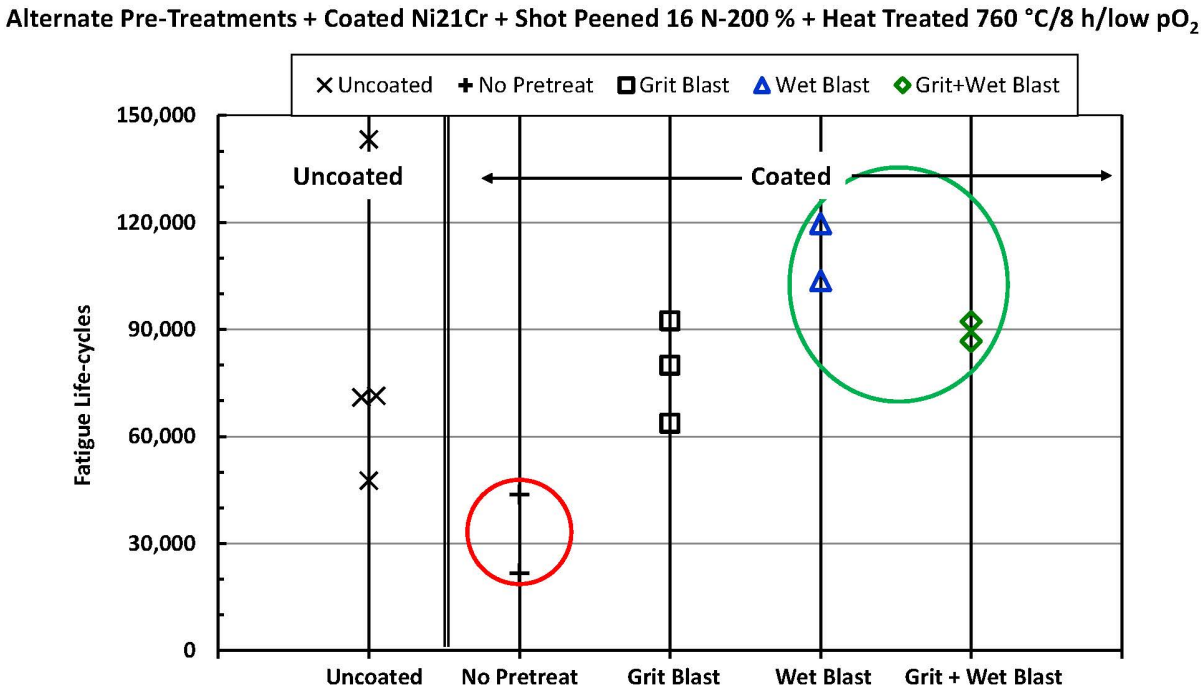

Figure 12.—Uncoated fatigue life versus coated fatigue lives after different pre-treatments, with no subsequent oxidation plus corrosion.

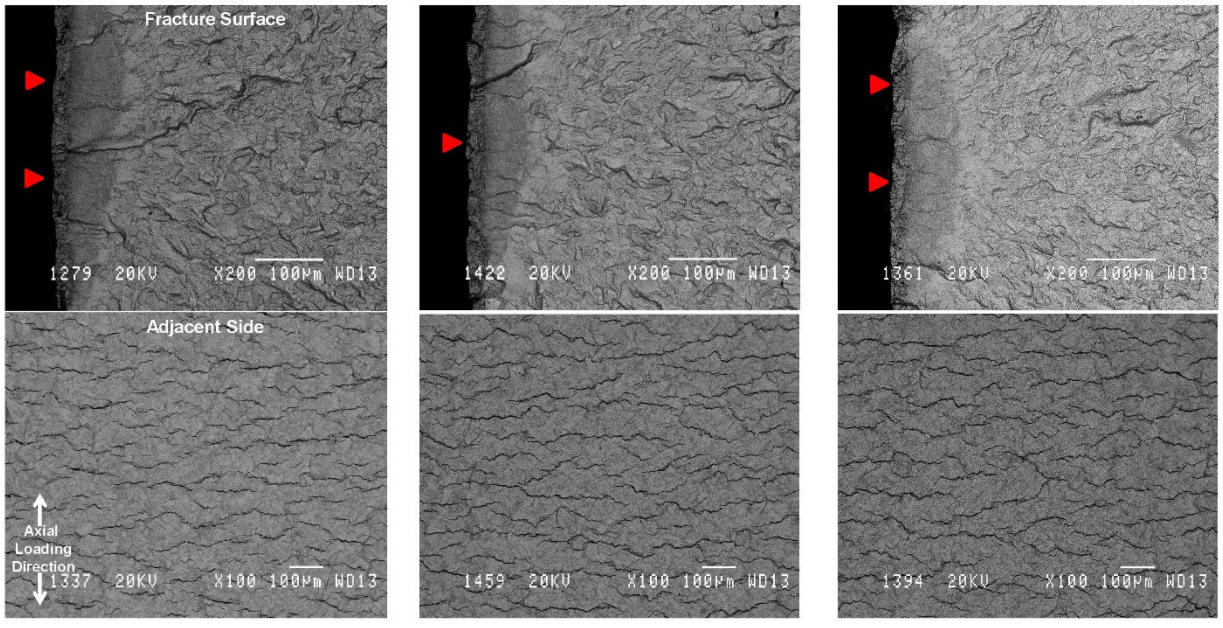

(a) (b) (c)

Figure 13.—Associated fatigue failure modes of coated specimens after different pre-treatments, no subsequent oxidation plus corrosion. (a) Grit blast. (b) Wet blast. (c) Grit plus wet blast. Coating crack density is comparable for the three cases.

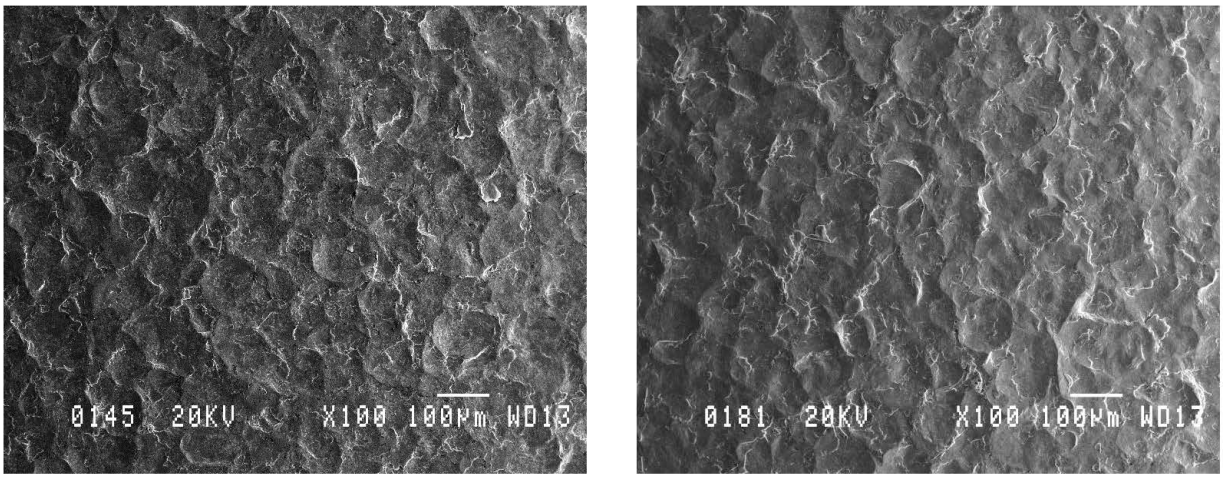

(a) (b)

Figure 14.—Images of coated specimens after different post-coating shot peening treatments, no subsequent oxidation plus corrosion. (a) 16 N-200%. (b) 8 N-150%. The fatigue loading direction is oriented vertically.

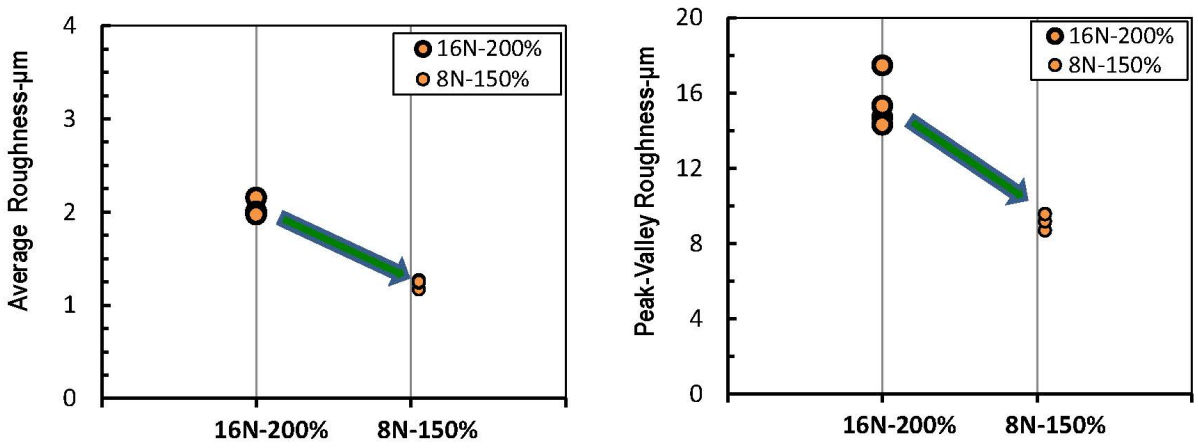

(a) (b)

Figure 15.—Associated roughness measurements of coated specimens after different post-coating shot peening treatments, no subsequent oxidation plus corrosion. (a) Average roughness. (b) Peak-valley roughness.

The axial residual stresses measured at the surface are compared in Figure 16. Shot peening at 8 N-150% gave a 35% lower magnitude of axial compressive residual stress on the coated surface, in comparison to the baseline 16 N-200% condition. The corresponding X-ray peak width has often been related to the plasticity (cold work) generated by shot peening (Refs. 14 and 18). This was therefore measured, and was curiously found to be slightly higher after 8 N-150% shot peening condition than for the baseline 16 N-200% condition. This implied slightly higher plasticity generated by shot peening at 8 N-150% than for 16 N-200%.

Nevertheless, final heat treatment at 760 °C for 8 h relaxed compressive surface residual stresses and corresponding peak width for both shot peening conditions to comparable levels at the coated surfaces, Figure 16. Heat treated coated specimens had modest tensile residual stresses of 350 to 450 MPa at the surface for both shot peening conditions. The generation of compressive residual stresses in the coating by shot peening has also been described for MCrAlY coatings applied by various processes (Ref. 20) and for NiCr coatings on superalloys (Ref. 21). Yet, evaluations of residual stress for a similar NiCrY coating with the baseline 16 N-200% shot peening and heat treatment indicated that significant compressive residual stresses of over –400 MPa remained at depths of up to 150 µm in this superalloy beneath the coating (Ref. 22). Therefore, the overall mechanics of the residual stress response at the surface can be

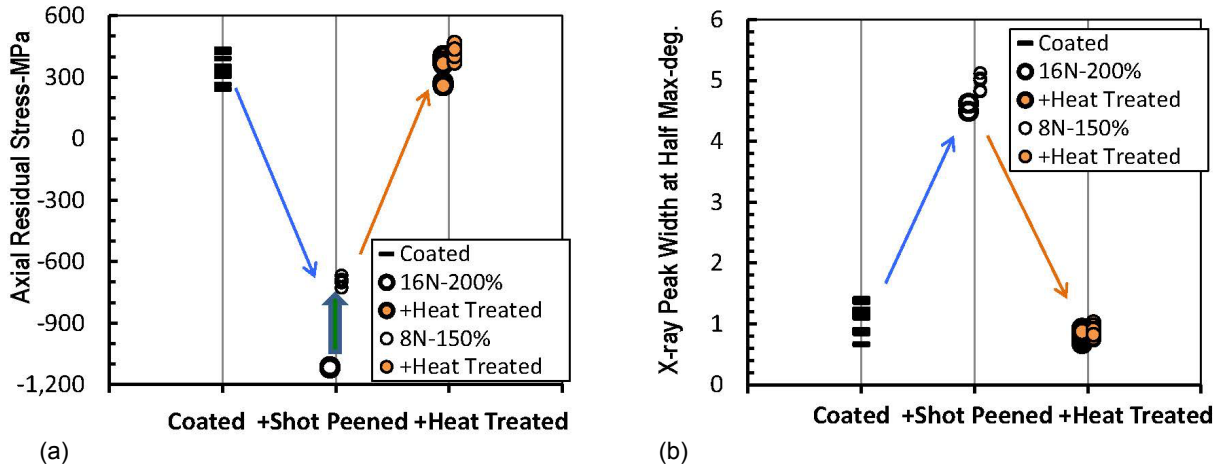

Figure16.—Associated x-ray measurements of coated specimens after different post-coating shot peening conditions, no subsequent oxidation plus corrosion. (a) Axial residual stress, relaxed to low tensile values after heat treatment from either shot peening condition. (b) Peak width at half maximum intensity, indicating elimination of shot peening's cold work after heat treatment from either shot peening condition.

attributed to the coating, and appears to be influenced by the low strength, lower stress relaxation resistance, and higher thermal contraction measured for such coatings in comparison to the superalloy substrate (Ref. 22).

Ranking these influences is more difficult, but can be aided by further considering the plasticity introduced by shot peening. Corresponding x-ray peak width was also greatly reduced by the heat treatment as shown in Figure 16. Peak width was reduced to actually equal that measured after only applying the coating. This implied the shot peening-induced plasticity had been largely eliminated by the heat treatment, through an enhanced recovery process occurring in the coating. Prior tensile stress relaxation tests of Nichrome specimens having a composition quite close to the coating indicated very low strength and accelerated stress relaxation of this alloy and coating (Ref. 22). So of the influences listed above, the impressive relaxation of compressive residual stresses in such NiCr coatings appears largely attributable to the low strength and an enhanced recovery – stress relaxation process in the coating at temperatures near 760 °C. The higher thermal contraction also previously measured (Ref. 22) for this alloy may then generate the low tensile stresses during cooling to room temperature, where residual stress measurements were conducted by x-ray diffraction.

Fatigue Lives and Failure Modes

Fatigue lives are compared in Figure 17 after varied pre-treatments, coating, 8 N-150% shot peening, heat treatment, and finally the combined oxidation plus corrosion exposures at 760 °C. The alternative pre-coating and post-coating treatments gave modestly improved coated fatigue lives after subsequent oxidation plus corrosion. Nevertheless, the coating could still be considered successful with the alternative conditions, enabling twice the fatigue life of uncoated specimens after combined oxidation and hot corrosion. Specimens with a final wet blasting treatment before coating and shot peening at 8 N-150% performed most favorably.

Typical images of the fracture surfaces for these fatigue failures are shown in Figure 18. Surface cracks initiated fatigue failures in all cases. Examination of the gage sides adjacent to the main failure initiation points indicated increased surface cracking in the coating still predominated, after pre-coating treatments of grit blasting and/or wet blasting and post-coating shot peening at 8 N-150% plus the standard heat treatment. The hot corrosion attack did not appear to form pits to expose the substrate for coated specimens with any combination of the pre-coating and post-coating treatments. However, patches of oxide were observed on the coating, and these patches sometimes had evidence of spallation and cracking.

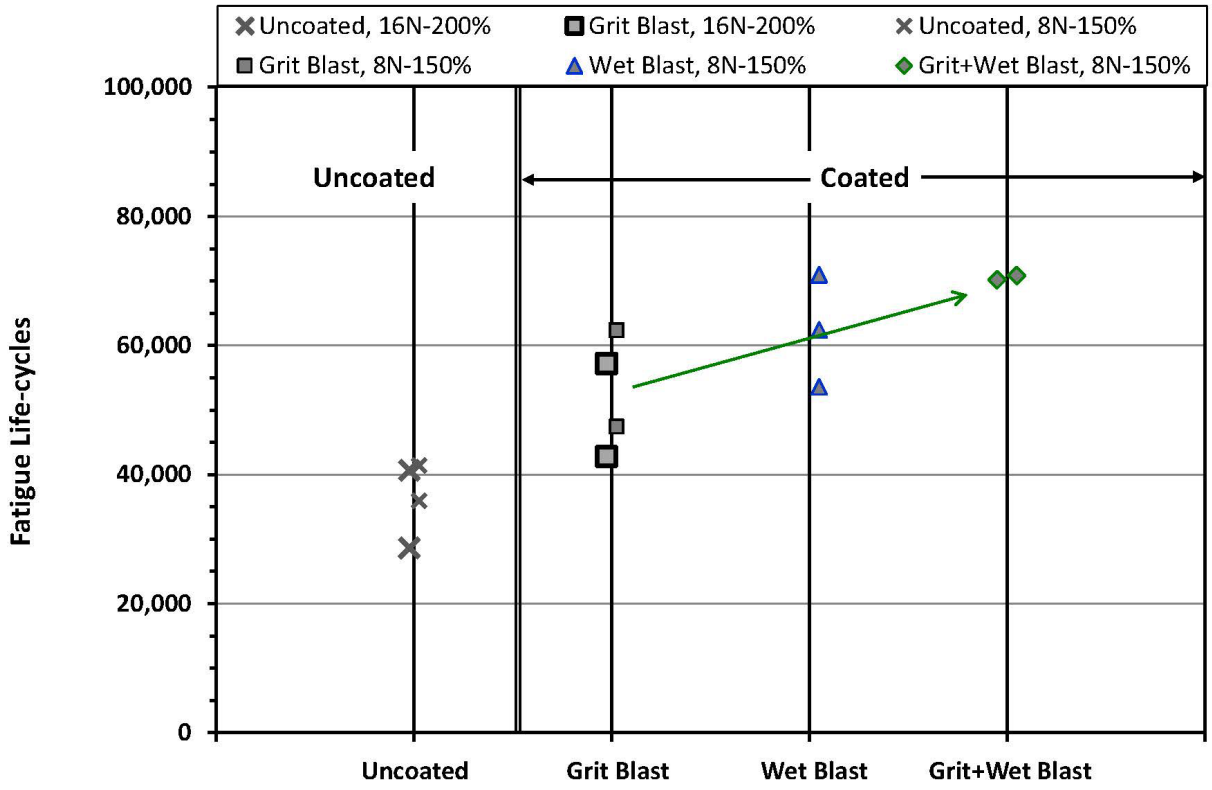

Figure 17.—Comparison of fatigue lives for alternative pre-coating and post-coating treatments, after oxidation plus corrosion. Larger symbols indicate baseline (16 N-200%) post-coat shot peen treatment, while smaller symbols indicate alternative (8 N-150%) post-coat shot peen treatment.

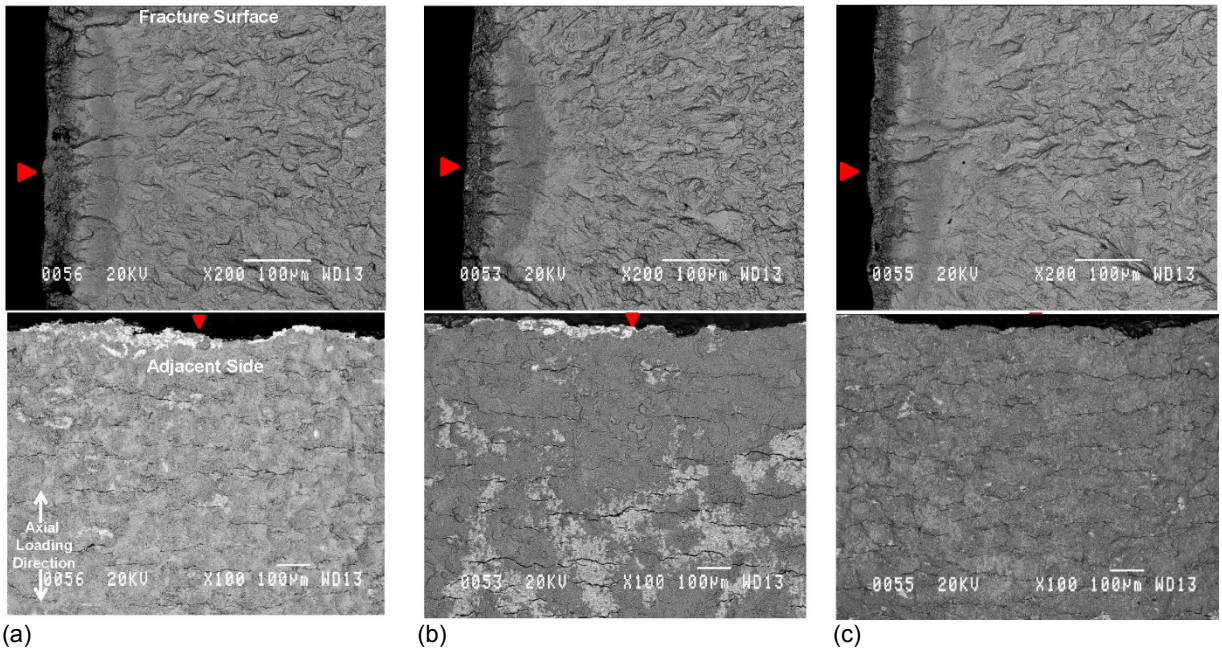

(a) (b) (c)

Figure 18.—Comparison of fatigue failure modes for alternative pre-coating and post-coating treatments, after oxidation plus corrosion. (a) Grit blast. (b) Wet blast. (c) Grit plus wet blast. Shot peened 8 N-150%.

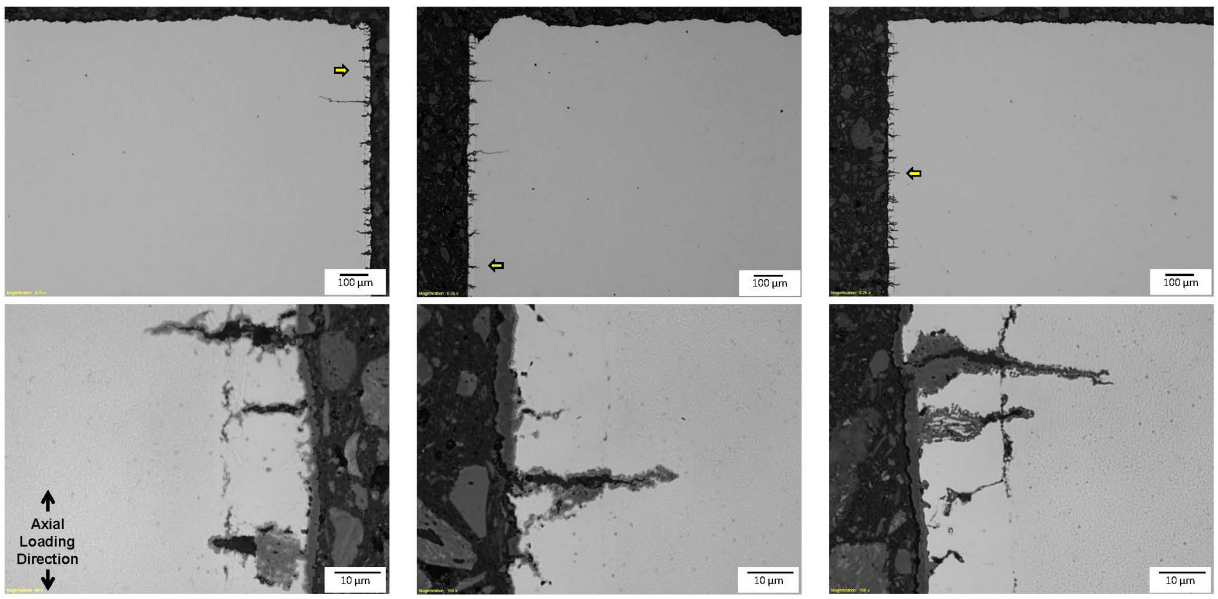

(a) (b) (c)

Figure 19.—Comparison of metallographically-prepared longitudinal sections for the failure initiation sites with alternative pre-coating and post-coating treatments, after oxidation plus corrosion. (a) Grit blast. (b) Wet blast. (c) Grit plus wet blast. All were coated, then shot peened 8 N-150% + heat treated 760 °C/8 h/low pO2 + oxidized 760 °C/500 h + hot corroded 760 °C/50 h before fatigue at 760 °C.

Metallographically prepared longitudinal cross-sections of these specimens are shown for comparison in Figure 19. The polishing plane for these test specimens was parallel to the loading direction. Multiple secondary fatigue cracks grew through the coating, but a majority did not extend into the underlying superalloy. The coating is still adhered well to the substrate, and is not lifted away at the cracks. Therefore, these cracks do not appear associated with "rumpling" of the coating due to excessive compressive creep there, as reported for plasma-sprayed MCrAlY overlay coatings on airfoil superalloys (Ref. 12). Rather, they appear to simply be tensile cracks in the weak NiCr coating. No corrosion pits penetrating through the coating to the substrate were found in these sections. Therefore, the coating did appear to protect the substrate superalloy from corrosion attack and pit formation after extended oxidation exposures, while preserving fatigue life when favorably pre-treated with wet blasting, then shot peened and heat treated after coating.

While roughness was reduced by the gentler alternative shot peening conditions of 8 N-150%, after heat treatment the residual stresses and cold work measured at the coating surface were comparable to those measured using the baseline shot peening of 16 N-200%. This indicated that the change in roughness was not a significant determinant for fatigue life, and that other factors were more important. Quite comparable fatigue cracking of the coating, but not the superalloy substrate, has been observed in studies of a similar γ+α phase Ni45CrY coating subjected to this processing and exposures on LSHR (Ref. 22). This was observed in fatigue without exposures and also after oxidation plus corrosion exposures. Attendant measurements of residual stress versus depth after interrupted fatigue cycling of these specimens indicated residual stresses at the surface of coated specimens became slightly tensile after the heat treatment, and remained so with continued fatigue cycling. Yet, significant compressive residual stresses remained below the coating in the adjacent superalloy substrate after heat treatment, and after extended fatigue cycling (Ref. 22).

It is apparent that a very similar situation could exist for the present NiCr-coated specimens. In spite of applying a more ductile single phase γ coating, using varied pre-treatments before coating, and varied shot peening conditions after coating, increased fatigue cracking continued to occur in the coating. This is consistent with the comparable tensile residual stresses measured in the coating after final heat treatment, which remained so for coated specimens not oxidized or corroded but fatigue tested for 700 fatigue cycles

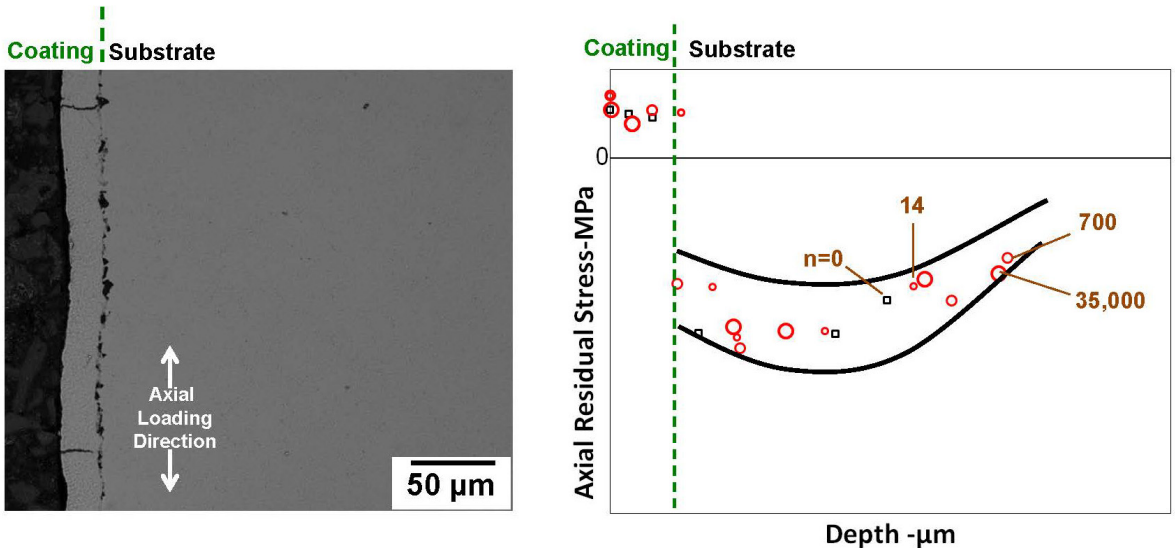

(a) (b)

Figure 20.—Ni45CrY-coated LSHR fatigue specimen (baseline process) tested at 760 °C/35,000 cycles. (a) Longitudinal section, showing fatigue cracking of the coating. (b) Measured axial residual stresses versus depth for specimens interrupted after up to 35,000 cycles (n) (Ref. 22) Baseline process used grit blast plus Ni45CrY coating plus shot peen 16 N-200% plus heat treat 760 °C for 8 h in low pO_2.

and for 35,000 cycles as shown in Figure 20. Yet, these fatigue cracks in the coating are clearly impeded from growing into the substrate, for specimens that had been coated, shot peened at either 16 N-200% (Ref. 17) or 8 N-150% (Fig. 19), and then heat treated, oxidized, and corroded. While no intact coated specimens of the present study remained for measuring residual stress as a function of depth, the evidence strongly suggests that axial compressive residual stresses remained in the superalloy substrate adjacent to the coating, to again suppress fatigue crack growth there.

The implications of such coating fatigue cracks on subsequent hot corrosion protection of the coating need to be further considered. Turbine engine disk components could be subjected to corrosion attack throughout the service life, when coating cracks could be present. Initial trials on Ni45CrY-coated specimens that had been fatigue cycled to produce coating cracks indicated the cracked coating can still protect the substrate in subsequent corrosion tests (Ref. 22). To confirm this for the present coating, additional tests would be necessary of NiCr-coated specimens that have been fatigue cycled for varied intervals, and then oxidation and corrosion tested.

Summary of Results

A baseline process path was evaluated of grit blasting and applying a ductile NiCr coating onto fatigue specimens of a disk superalloy, then shot peening and heat treating them. Shot peening suppressed "spits" on the coating surface while increasing average roughness, but the induced compressive residual stresses at the surface relaxed during subsequent heat treatment. Coated and uncoated specimens were fatigue tested at 760 °C, some after oxidation plus hot corrosion exposures. Uncoated specimens had significant reductions in fatigue life, due to fatigue failures initiated from corrosion pits. Coated specimens had no distinct corrosion pits formed and lower reductions in fatigue life, yet increased surface cracking occurred in the coating. Alternative surface pre-treatments were screened, and improvements in fatigue life were indicated for wet blast coated specimens, though increased fatigue cracking of the coating still predominated. Alternative shot peening conditions were screened after coating, yet the fatigue lives after exposures were only modestly improved, and increased surface cracking of coated specimens remained. Examinations of metallographically prepared longitudinal sections of the coated specimens with and without exposures before fatigue testing indicated the secondary coating cracks observed on the gage sides more often did not grow into the superalloy substrate.

Conclusions

1. Effects of baseline coating process on disk superalloy fatigue life at 760 °C: NiCr coatings can improve fatigue life in applications where oxidization plus hot corrosion are expected to occur. Without these exposures, fatigue life of properly processed coated specimens can be comparable to that of uncoated specimens. However, increased fatigue cracking of the coating can occur.
2. Varied surface pre-treatments before coating: Wet blasting can imbed less ceramic particles than for baseline grit blasting and modestly improve coated fatigue life, but will not eliminate increased fatigue cracking of the coating.
3. Varied shot peening after coating: Reduced shot peening intensity and coverage values near those examined here can reduce roughness, but not significantly change surface residual stress and peak width eventually stabilized after heat treatment, and will not eliminate increased fatigue cracking of the coating.
4. Why there can be increased fatigue cracking of the coating, yet good fatigue lives even after exposures: Fatigue cracks can form sooner in NiCr γ phase and $\gamma + \alpha$ phase coatings, where no compressive residual stresses from shot peening remain after heating near 760 °C. However, the substrate below the coating can still retain some compressive residual stresses, to help suppress crack growth there.

References

1. R. Schafrik, R. Sprague, "Superalloy Technology–A Perspective on Critical Innovations for Turbine Engines," Key Engineering Materials, V 380, 2008, pp. 113–134.
2. M.R. Bache, J.P. Jones, G.L. Drew, M.C. Hardy, N. Fox, "Environment and Time Dependent Effects on the Fatigue Response of an Advanced Nickel Based Superalloy," Int. J. Fat., V 31 (11-12), 2009, pp. 1719–1723.
3. A. Encinas-Oropesa, G. Drew, M. Hardy, A. Leggett, J. Nicholls, and N. Simms, "Effects of Oxidation and Hot Corrosion in a Nickel Disc Alloy," Superalloys 2008, ed. R.C. Reed, K.A. Green, P. Caron, T.P. Gabb, M.A. Fahrmann, E.S. Huron, S.A. Woodard, The Mining, Metallurgy, and Materials Society, Warrendale, PA, 2008, pp. 609–618.
4. C.K. Sudbrack, S.L. Draper, T. Gorman, J. Telesman, T.P. Gabb, D.R. Hull, "Oxidation and the Effects of High Temperature Exposures on Notched Fatigue Life of an Advanced Powder Metallurgy Disk Superalloy," Superalloys 2012, E.S. Huron, R.C. Reed, M.C. Hardy, M.J. Mills, R.E. Montero, P.D. Portella and J. Telesman, Eds., TMS, Warrendale, PA, 2012, pp. 863–872.
5. R.A. Rapp, "Hot Corrosion of Materials: A Fluxing Mechanism?", Corrosion Sci., 2002, 44, pp. 209–221.
6. F.S. Pettit and C.S. Giggins, "Hot Corrosion," Superalloys II, C.T. Sims, N.S. Stoloff, and W.C. Hagel, Eds., John Wiley & Sons, New York, 1987, pp. 327–358.
7. B. Gleason, "High-Temperature Corrosion of Metallic Alloys and Coatings," Materials Science and Technology, ed. R.W. Cahn, P. Haasen, E.J. Kramer, John Wiley & Sons Inc., 2000, pp. 173–228.
8. J.R. Groh and R.W. Duvelius, "Influence of Corrosion Pitting on Alloy 718 Fatigue Capability," Superalloy 718, 625, 706 and Derivatives, ed. E.A. Loria, The Mining, Metallurgy, and Materials Society, Warrendale, PA, 2001, pp. 583–592.
9. G.S. Mahobia, N. Paulose, S.L. Mannan, R.G. Sudhakar, K. Chattopadhyay, N.C.S. Srinivas, "Effects of Hot Corrosion on the Low Cycle Fatigue Behavior of IN718," Int. J. Fat., V. 59, 2014, pp. 272–281.
10. J.K. Sahu, R.K. Gupta, J. Swaminathan, N. Paulose, S.L. Mannan, "Influence of Hot Corrosion on the Low Cycle Fatigue Behavior of SU 263," Int. J. Fat., V. 51, 2013, pp. 68–73.
11. J. Telesman, T.P. Gabb, Y. Yamada, S.L. Draper, "Fatigue Resistance of a Hot Corrosion Exposed Disk Superalloy at Varied Test Temperatures," Mat. at High Temperatures, V. 33 (4-5), 2016, pp. 517–527.

12. G.W. Goward, “Progress in Coatings for Gas Turbine Airfoils,” Surface and Coatings Technology, V. 108–109, 1998, pp. 73–79.
13. D.R. Chang, D.D. Krueger, R.A. Sprague, “Superalloy Powder Processing, Properties and Turbine Disk Applications,” Superalloys 1984, ed. M. Gell, C.S. Kortovich, R.H. Bricknell, W.B. Kent, J.F. Radavich, The Minerals, Metals & Materials Society, Warrendale, PA, 1984, pp. 245–273.
14. P.S. Prevéy “X-Ray Diffraction Characterization of Residual Stresses Produced by Shot Peening,” Shot Peening Theory and Application, ed. A. Niku-Lari, IITT-International, Gournay-Sur-Marne, France, 1990, pp. 81–93.
15. M.K. Tufft, “Shot Peen Impact on Life, Part 1: Development of a Fracture Mechanics/Threshold Behavior Predictive Model,” Shot Peening Present & Future, Proc. Of the 7th International Conference on Shot Peening, Institute of Precision Mechanics, 1999, pp. 244–253.
16. G. Kappmeyer, C. Hubig, M. Hardy, M. Witty, M. Busch, “Modern Machining of Advanced Aerospace Alloys – Enabler for Quality and Performance,” 5th CIRP Conference on High Performance Cutting 2012, Elsevier B.V., Amsterdam, The Netherlands, 2012, pp. 28–43.
17. T.P. Gabb, R.A. Miller, J.A. Nesbitt, S.L. Draper, R.B. Rogers, J. Telesman, “The Effectiveness of a NiCrY-Coating on a Powder Metallurgy Disk Superalloy,” NASA/TM—2018-219885, Washington, D.C., April, 2018.
18. J.T. Cammet, P.S. Prevéy, N. Jayaraman, “The Effect of Shot Peening Coverage on Residual Stress, Cold Work, and Fatigue in a Nickel-Base Superalloy,” Proceedings of ICSP 9, 2005.
19. J. Nesbitt, S.L. Draper, “Pit Morphology and Depth after Low-temperature Hot Corrosion of a Disc Alloy,” Mat. at High Temperatures, V. 51 (4-5), 2016, pp. 501–516.
20. J.F. Loersch, J.W. Neal, “Peened Overlay Coatings,” U. S. 4,514,469, U. S. Patent Office, Washington, DC, 1985.
21. B.T. Hazel, M.J. Weimer, “Turbine Component Protected With Environmental Coating,” U.S. 7,364,801 B1, U. S. Patent Office, Washington, DC, 2008.
22. T.P. Gabb, R.B. Rogers, J.A. Nesbitt, R.A. Miller, B.J. Puleo, D. Johnson, J. Telesman, S.L. Draper, I.E. Locci, “Influences of Processing and Fatigue Cycling on Residual Stresses in a NiCrY-Coated Powder Metallurgy Disk Superalloy,” J. Mat. Eng. Perf., V. 26(11), 2017, pp. 5237–5250.
23. L.H. Burck, C.P. Sullivan, C.H. Wells, “Fatigue of a Glass Bead Blasted Nickel-base Superalloy,” Met. Trans. B, V. 1(6), 1970, pp. 1595–1600.